JOURNAL OF MATERIALS SCIENCE 14 (1979) 205–220

Differential geometry of the coincidence site lattice*

M. J. MARCINKOWSKI
Engineering Materials Group, and Department of Mechanical Engineering, University of Maryland, College Park, Maryland 20742, USA

The tensor properties of simple internal surfaces, such as two-phase interfaces and grain boundaries, have been studied in detail. In particular, these tensor quantities have been defined with respect to the original crystal lattice as well as to a common coincidence site lattice that is a characteristic of the boundary. Such lattices allow a given type of distortion to be represented in either a Riemannian or a non-Riemannian (dislocated) space. This particular generality provides a powerful method of anlysing problems in continuum mechanics.

1. Introduction

The coincidence site lattice description of a grain boundary [1] and a two-phase interface [2] has already been formulated in relatively simple terms. Since many of the concepts developed therein appear to be quite fundamental with respect to a more generalized theory of dislocations, it was felt that a reformulation of these concepts in terms of the language of differential geometry would provide the required theoretical framework.

2. Distortions associated with a two-phase interface

Consider two simple cubic crystals of differing lattice constant a_0 and b_0 belonging to phases A and B respectively. If they are joined together so that the crystallographic planes are continuous across the interface, the configuration shown in Fig. 1 is obtained. Such a boundary is fully coherent and may be visualized in terms of a vertical array of virtual edge dislocations shown by the dotted symbols, each of strength $a_0 - b_0$ as first described by Marcinkowski [3]. As we shall shortly see, such a description is not strictly correct geometrically, since no extra half planes are present. In fact, the distortion is actually elastic and will be designated by lower case Greek letters, i.e., κ, λ, etc.

The fully coherent boundary of Fig. 1 can now be made completely non-coherent by the introduction of an extra half plane, i.e., edge dislocation, every five interatomic spacings, measured in terms of phase B, as shown in Fig. 2. These are represented by the solid dislocation symbols and are

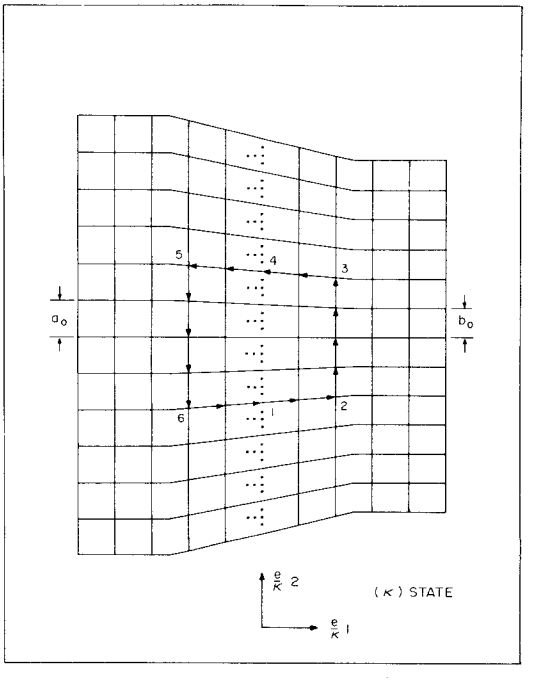

Figure 1 Fully coherent interphase boundary.

*The present research was supported by the National Science Foundation under Grant no. DMR–7202944.

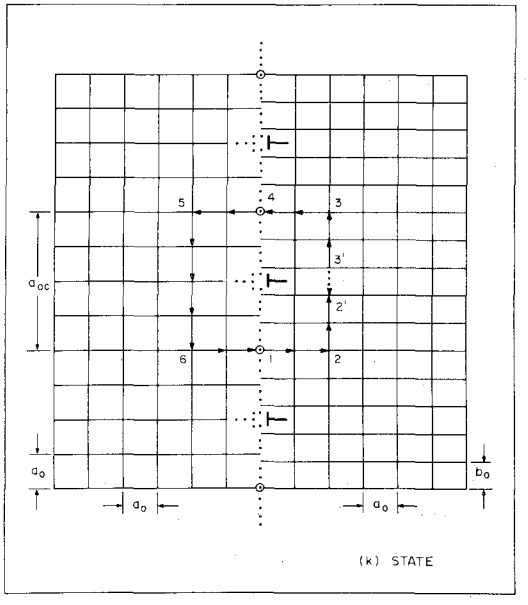

Figure 2 Fully compensated interphase boundary.

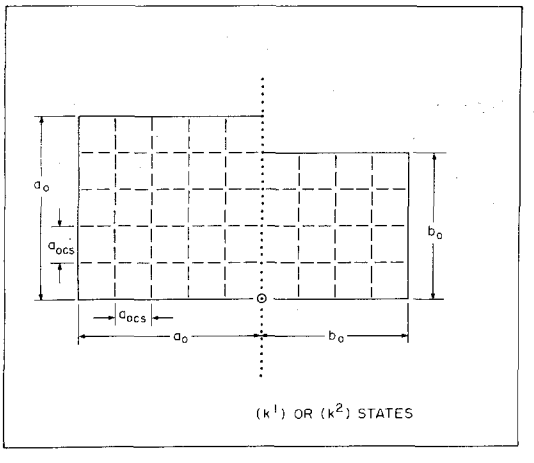

Figure 3 Coincidence site sublattice associated with the interface boundary of Fig. 2.

seen to completely compensate the virtual dislocations associated with the fully coherent boundary. We shall represent the completely compensated state in Fig. 2 by lower case Roman letters, i.e., k, l, etc.

Inspection of Fig. 2 shows that the interphase boundary contains a number of coincidence sites which are shown as open circles. These sites generate a coincidence site lattice of edge dimensions a_{oc} which is common to both phases and in terms of this description may be labelled as state (k^1). The coincidence site lattice unit cells can in turn be subdivided into a still smaller sublattice of unit cell edge length a_{ocs}, as outlined by the

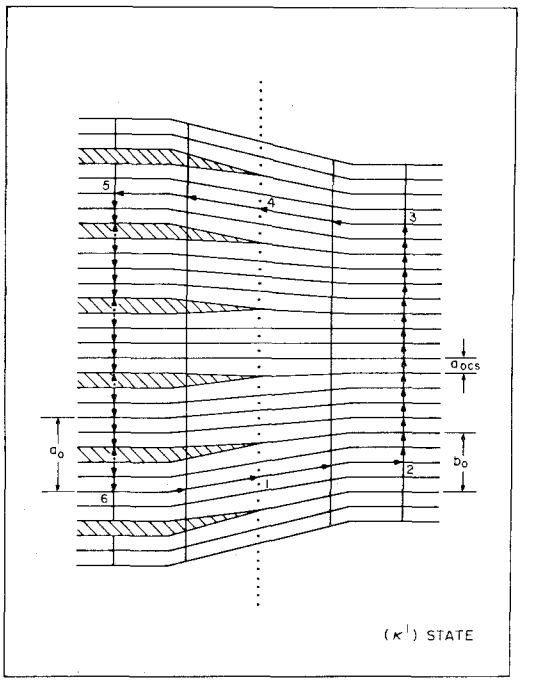

Figure 4 Description of Fig. 1 in terms of the coincidence site lattice sublattice.

dashed lines of Fig. 3. This particular designation will be denoted as state (k^2). It is apparent from this figure that a_{ocs} is simply equal to $a_0 - b_0$ and provides still more physical insight into the coherent boundary of Fig. 1. In particular, when the (κ) state is redrawn in terms of the coincidence site lattice sublattice, the configuration denoted as state (κ^1) in Fig. 4 is obtained. In particular, it is seen to consist of an array of extra half planes (shown shaded) of strength a_{ocs} spaced every five coincidence site lattice sublattice unit cell distances. This, in fact, is the correct dislocation model of the coherent dislocation model of the coherent boundary of Fig. 1 and is the true origin of the dotted dislocations which were originally termed virtual dislocations. We see, however, that in terms of Fig. 4, the dislocations are, in fact, real ones, so that strictly speaking the (κ) state is an undislocated state.

The various states (κ), (k), (k^1), (k^2), and (κ^1), as well as (K), (k^3), (k^4), and (K^1) which will be considered later, can all be connected to one another. For example, the transitions $(K) \rightarrow (k)$, $(K) \rightarrow (k^1)$, $(K) \rightarrow (k^2)$, $(k) \rightarrow (k^1)$, $(k) \rightarrow (k^2)$, $(k^1) \rightarrow (k^2)$, $(\kappa) \rightarrow (\kappa^1)$, and $(K) \rightarrow (K^1)$ correspond simply to coordinate transformations or reference frame changes. On the other hand, the transformations $(K) \rightarrow (\kappa)$, $(k^2) \rightarrow (\kappa^1)$, $(\kappa) \rightarrow (k)$,

$(K) \rightarrow (k^3)$, $(\kappa) \rightarrow (k^3)$, $(\kappa^1) \rightarrow (k^4)$, and $(k) \rightarrow (k^3)$ correspond to distortions or changes in state. According to Schouten's notation, [4] only reference frames are enclosed in parentheses; however, this should not lead to any difficulties in the subsequent analysis, when the above correspondences are kept in mind. The various transformation tensors can now be used to write

$$dx^{k} = C^{k}_{K}\, dx^{K} \tag{1a}$$

$$dx^{\kappa^1} = C^{\kappa^1}_{\kappa}\, dx^{\kappa} \tag{1b}$$

etc., and

$$e_{k} = C^{K}_{k}\, e_{K} \tag{2a}$$

$$e_{\kappa^1} = C^{\kappa}_{\kappa^1}\, e_{\kappa} \tag{2b}$$

etc., where e_{κ}, etc., are base vectors, while dx^{κ}, etc., are components associated with the vectors. The C^{k}_{K} and their inverses C^{K}_{k} are related according to

$$C^{k}_{K}\, C^{K}_{l} = \delta^{k}_{l} \tag{3}$$

where δ^{k}_{l} is the Kronecker delta.

In the case of the distortions, we shall first consider those that are elastic in nature, i.e., $(K) \rightarrow (\kappa)$. The corresponding distortion tensor can be written as B^{K}_{κ} from which [5]

$$e_{\kappa} = B^{K}_{\kappa}\, e_{K}. \tag{4}$$

A perfect lattice, such as shown in Fig. 5, will be chosen as a reference state and denoted by upper case Latin letters, i.e., K, L, etc. The distortion in Fig. 1 can be written as follows

$$B^{K}_{\kappa} = \begin{pmatrix} B^1_1 & B^2_1 & B^3_1 \\ B^1_2 & B^2_2 & B^3_2 \\ B^1_3 & B^2_3 & B^3_3 \end{pmatrix} = \begin{pmatrix} 1 & B^2_1 & 0 \\ 0 & B^2_2 & 0 \\ 0 & 0 & 1 \end{pmatrix} \tag{5}$$

where

$$B^2_2 = f_1 + V f_2 \tag{6}$$

and where f_1 and f_2 are defined as

$$f_1 = [\exp(a \underset{K}{x}{}^1) + 1]^{-1} \tag{7}$$

and

$$f_2 = [\exp(-a \underset{K}{x}{}^1) + 1]^{-1} \tag{7b}$$

where the coordinate $\underset{K}{x}{}^1$ is measured with respect to the local coordinate system at the potential boundary shown dotted in Fig. 5. Thus, for

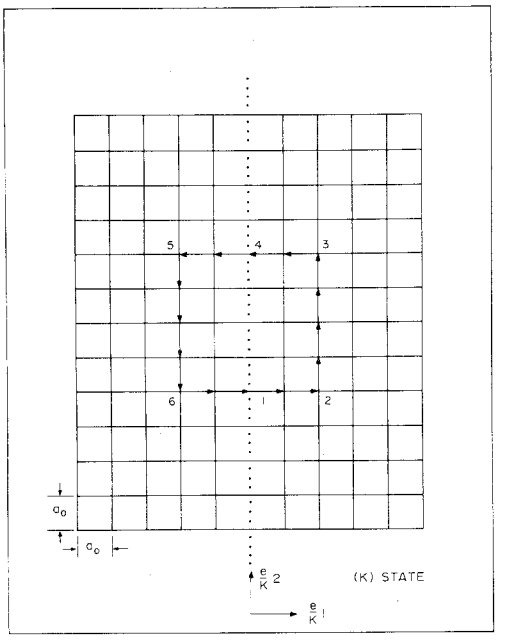

Figure 5 Perfect lattice reference state.

$\underset{K}{x}{}^1 \rightarrow -\infty$, $f_2 = 0$ and $B^2_2 = f_1 = 1$, while for $x^1 \rightarrow +\infty$, $f_1 = 0$ and $B^2_2 = f_2 = V$. Right at the boundary, where $\underset{K}{x}{}^1 = 0$, $B^2_2 = (1 + V)/2$. Fig. 1 was drawn with $V = 4/5$, i.e., $b_o = 4/5\, a_o$. The component B^2_1 in Equation 5 is some suitable function which gives the vertical displacement of the horizontal planes in Fig. 1. In particular, it can be written as

$$B^2_1 = x^2\, \partial_1 B^2_2. \tag{8}$$

Thus, the function given by Equation 6 seems to be an appropriate one, where the parameter a can be chosen so as to adjust the width of the distorted zone across the boundary. Also tacitly assumed in Equation 6 is that b_o is attained by an elastic distortion V of a_o. Thus, Equation 6 can be written out in full as

$$B^2_2 = [1 + V \exp(a \underset{K}{x}{}^1)]/[1 + \exp(a \underset{K}{x}{}^1)] \tag{9}$$

while the inverse quantity B^{κ}_{K} can be simply found from the following relation:

$$B^{\kappa}_{K}\, B^{K}_{\lambda} = \delta^{\kappa}_{\lambda}. \tag{10}$$

For simplicity, both B^1_1 and B^3_3 were chosen equal to 1 in Equation 5. In any event, we can now use Equation 10 to write for $\bar{B}^2_2$

$$\bar{B}^2_2 = [1 + \exp(a \underset{K}{x}{}^1)]/[1 + V \exp(a \underset{K}{x}{}^1)] \tag{11}$$

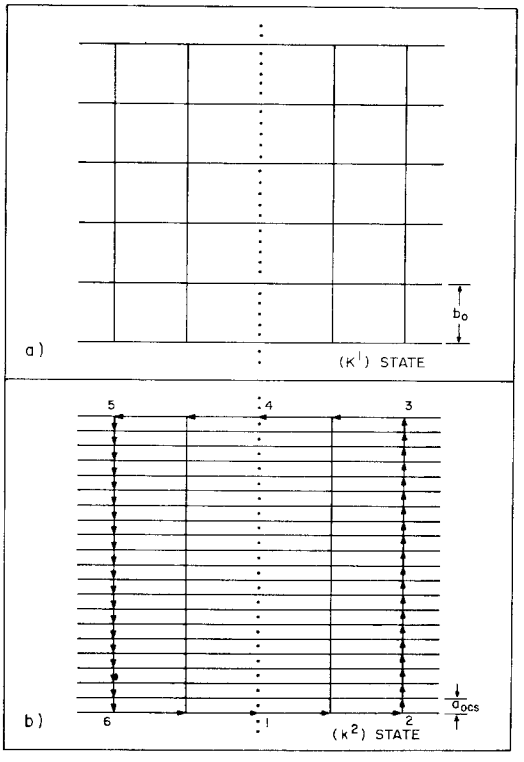

Figure 6 States generated from the (K) state of Fig. 5.

where the bar over B denotes that the terms are of the form B^{κ}_{K}, i.e., the inverse distortions.

In order to properly represent the distortion $(\mathrm{K}) \rightarrow (\kappa)$, it is important to note that we must not write

$$\mathrm{d}x^{\kappa} = B^{\kappa}_{\mathrm{K}}\, \mathrm{d}x^{\mathrm{K}} \tag{12a}$$

but instead

$$\mathrm{d}x^{\kappa} = \delta^{\kappa}_{\mathrm{K}}\, \mathrm{d}x^{\mathrm{K}}. \tag{12b}$$

Under the conditions imposed by Equation 12b, the coordinates retain their same numerical values in both states, i.e., they are dragged along by the transformation [4]. As will also be shown in the following section, this formulation is also compatible with the proper definition of strain.

Let us now consider the distortion given by $(\mathrm{k}^2) \rightarrow (\kappa^1)$ which involves dislocations. The k^2 state is shown in Fig. 6b. In this case, we can write the distortion as $A^{\kappa^1}_{\mathrm{k}^2}$, which gives

$$\mathrm{d}x^{\kappa^1} = A^{\kappa^1}_{\mathrm{k}^2}\, \mathrm{d}x^{\mathrm{k}^2} \tag{13}$$

and where

$$A^{\kappa^1}_{\mathrm{k}^2} = \{{}_1A^{\kappa^1}_{\mathrm{k}^2}\, H(-\underset{\mathrm{k}^2}{x^1})\}_1 + \{{}_2A^{\kappa^1}_{\mathrm{k}^2}\, H(+\underset{\mathrm{k}^2}{x^1})\}_2 \tag{14}$$

while

$$ {}_1A^{\kappa^1}_{\mathrm{k}^2} = \delta^{\kappa^1}_{\mathrm{k}^2} \tag{15a}$$

and

$$ {}_2A^{\kappa^1}_{\mathrm{k}^2} = \begin{pmatrix} 1 & 0 & 0 \\ 0 & V & 0 \\ 0 & 0 & 1 \end{pmatrix}. \tag{15b}$$

The quantities $H(-\underset{\mathrm{k}^2}{x^1})$ and $H(+\underset{\mathrm{k}^2}{x^1})$ are Heaviside functions defined by

$$H(-\underset{\mathrm{k}^2}{x^1}) = \begin{cases} 0 \text{ if } \underset{\mathrm{k}^2}{x^1} > 0 \\ 1 \text{ if } \underset{\mathrm{k}^2}{x^1} < 0 \end{cases} \tag{16a}$$

and

$$H(+\underset{\mathrm{k}^2}{x^1}) = \begin{cases} 0 \text{ if } \underset{\mathrm{k}^2}{x^1} < 0 \\ 1 \text{ if } \underset{\mathrm{k}^2}{x^1} > 0 \end{cases} \tag{16b}$$

where $\underset{\mathrm{k}^2}{x^1}$ is measured from the boundary. It is important to note from Equation 13 that the coordinates are not dragged when the strain is expressed in terms of dislocations. The curly bracket notation is used in Equation 14 to emphasize the fact that each phase may be treated separately.

For the coordinate transformation $(\mathrm{K}) \rightarrow (\mathrm{k})$, $C^{\mathrm{k}}_{\mathrm{K}}$ and $C^{\mathrm{K}}_{\mathrm{k}}$ given by Equations 1a and 2a respectively become

$$C^{\mathrm{k}}_{\mathrm{K}} = \{{}_1C^{\mathrm{k}}_{\mathrm{K}}\, H(-\underset{\mathrm{K}}{x^1})\}_1 + \{{}_2C^{\mathrm{k}}_{\mathrm{K}}\, H(+\underset{\mathrm{K}}{x^1})\}_2 \tag{17a}$$

and

$$C^{\mathrm{K}}_{\mathrm{k}} = \{{}_1C^{\mathrm{K}}_{\mathrm{k}}\, H(-\underset{\mathrm{K}}{x^1})\}_1 + \{{}_2C^{\mathrm{K}}_{\mathrm{k}}\, H(+\underset{\mathrm{K}}{x^1})\}_2 \tag{17b}$$

where

$$ {}_1C^{\mathrm{k}}_{\mathrm{K}} = \delta^{\mathrm{k}}_{\mathrm{K}} \tag{18a}$$

$$ {}_1C^{\mathrm{K}}_{\mathrm{k}} = \delta^{\mathrm{K}}_{\mathrm{k}} \tag{18b}$$

$$ {}_2C^{\mathrm{k}}_{\mathrm{K}} = \begin{pmatrix} 1 & 0 & 0 \\ 0 & 1/V & 0 \\ 0 & 0 & 0 \end{pmatrix} \tag{18c}$$

$$ {}_2C^{\mathrm{K}}_{\mathrm{k}} \equiv {}_2C^{\kappa^1}_{\mathrm{k}^2}. \tag{18d}$$

It is also interesting to note that the $(\mathrm{K}) \rightarrow (\mathrm{k})$

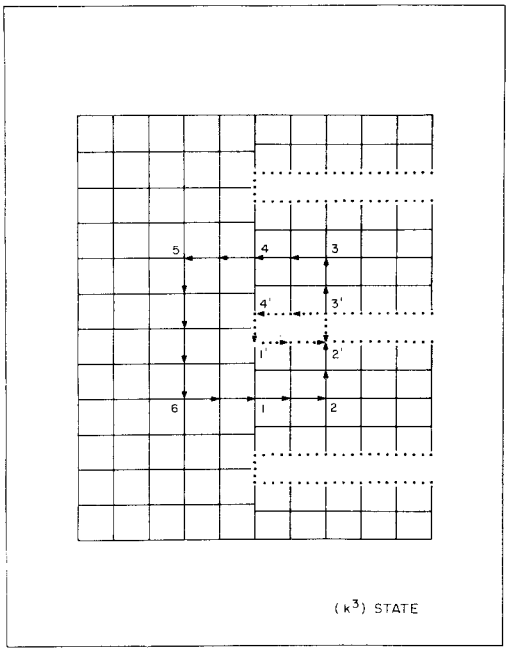

Figure 7 Configuration generated by tearing of the (κ) state of Fig. 1.

coordinate transformation could also be written as the two-step distortion (K) → (κ) → (k), so that

$$C_{\mathrm{K}}^{\mathrm{k}} = B_{\mathrm{K}}^{\kappa} A_{\kappa}^{\mathrm{k}} \tag{19}$$

where

$$A_{\kappa}^{\mathrm{k}} \equiv C_{\mathrm{K}}^{\mathrm{k}}. \tag{20}$$

The coordinate transformation (κ) → (κ^1) is also of interest and may be written as

$$\mathrm{d}x^{\kappa^1} = C_{\kappa}^{\kappa^1} \mathrm{d}x^{\kappa} \tag{21}$$

where

$$C_{\kappa}^{\kappa^1} = \{{}_1C_{\kappa}^{\kappa^1} H(-\underset{\kappa}{x}{}^1)\}_1 + \{{}_2C_{\kappa}^{\kappa^1} H(+\underset{\kappa}{x}{}^1)\}_2 \tag{22}$$

and where

$${}_1C_1^1 = {}_2C_1^1 = {}_1C_3^3 = {}_2C_3^3 = 1 \tag{23a}$$

$${}_1C_2^2 = 5 \tag{23b}$$

$${}_2C_2^2 = 4. \tag{23c}$$

Thus far we have denoted coordinate transformations by C, elastic distortions by B, i.e., (K) → (κ), and distortions involving dislocations, i.e., (k^2) → (κ^1) and (κ) → (k) by A. Let us now consider the process of tearing which removes all of the elastic distortions associated with the (κ) state configuration of Fig. 1. The resultant state is shown in Fig. 7 and will be denoted as (k^3). It is apparent that such tearing requires the formation of new surfaces, all of which are denoted by dotted lines in Fig. 7. The (k^3) state could also have been generated from the (K) state by means of the following distortion tensors

$$D_{\mathrm{k}^3}^{\mathrm{K}} = \{{}_1D_{\mathrm{k}^3}^{\mathrm{K}} H(-\underset{\mathrm{K}}{x}{}^1)\}_1 + \{{}_2D_{\mathrm{k}^3}^{\mathrm{K}} H(+\underset{\mathrm{K}}{x}{}^1)\}_2 \tag{24a}$$

and the inverse

$$D_{\mathrm{K}}^{\mathrm{k}^3} = \{{}_1D_{\mathrm{K}}^{\mathrm{k}^3} H(-\underset{\mathrm{K}}{x}{}^1)\}_1 + \{{}_2D_{\mathrm{K}}^{\mathrm{k}^3} H(+\underset{\mathrm{K}}{x}{}^1)\}_2 \tag{24b}$$

where

$${}_1D_{\mathrm{K}}^{\mathrm{k}^3} = \delta_{\mathrm{K}}^{\mathrm{k}^3} \tag{25a}$$

$${}_1D_{\mathrm{k}^3}^{\mathrm{K}} = \delta_{\mathrm{k}^3}^{\mathrm{K}} \tag{25b}$$

$${}_2D_{\mathrm{k}^3}^{\mathrm{K}} \equiv {}_2A_{\mathrm{k}^2}^{\kappa^1} \tag{25c}$$

as given by Equation 15b, while

$${}_2D_{\mathrm{K}}^{\mathrm{k}^3} \equiv {}_2C_{\mathrm{K}}^{\mathrm{k}} \tag{25d}$$

as given by Equation 18c. It is apparent that Equations 24a and 24b represent the limiting cases of Equations 6 and 11 respectively as a in the latter expressions approaches ∞. Important to note, however, is that the component $D_{\mathrm{I}}^{2} = 0$. Similar to Fig. 7, the dislocated (κ^1) state of Fig. 4 can be torn to generate the (k^4) state shown in Fig. 8. All of the tearing distortions, i.e., (K) → (k^3), (κ) → (k^3), (κ^1) → (k^4), and (k) → (k^3) will be noted by D. Similar to the case of Equation 12, the coordinates associated with the (K) → (k^3) distortion can be dragged by writing for Equation 25d, ${}_2D_{\mathrm{K}}^{\mathrm{k}^3} = \delta_{\mathrm{K}}^{\mathrm{k}^3}$. However, as we shall see later, the dragging concept cannot be applied right at the boundary, and we must use Equations 24 there. On the other hand, within the individual grains or phases, the dragging concept can be utilized, and under these conditions the (K) → (k) coordinate transformation can be written as a pair of sequential distortions (K) → (k^3) → (k) as follows

$$C_{\mathrm{K}}^{\mathrm{k}} = D_{\mathrm{K}}^{\mathrm{k}^3} A_{\mathrm{k}^3}^{\mathrm{k}} \tag{26}$$

where

$$A_{\mathrm{k}^3}^{\mathrm{k}} \equiv C_{\mathrm{K}}^{\mathrm{k}} \tag{27}$$

as given by Equation 17a. We thus see that coordinate transformations and distortions, whether they

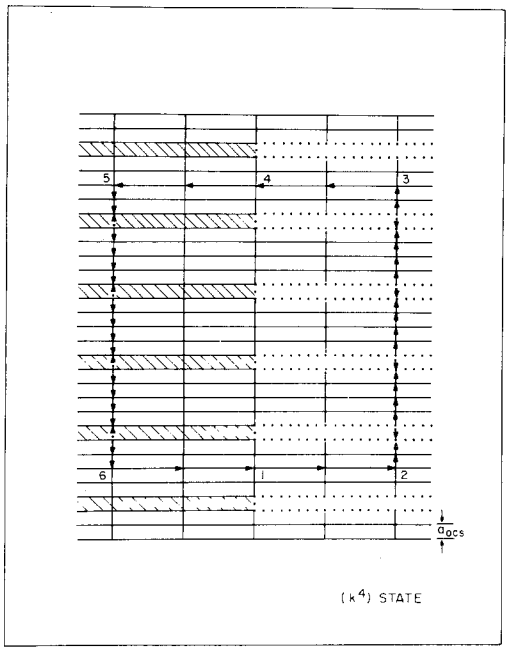

Figure 8 Configuration generated by tearing of the dislocated (κ^1) state crystal in Fig. 4.

be caused by elasticity, dislocations or tearing, are very closely related to one another.

3. Metric and strain tensors associated with a two-phase interface

We are now in a position to formulate expressions for the strain tensors associated with the distortions discussed in the previous section. In particular, for the elastic (K) → (κ) distortion [6]

$$e_{KL} = \tfrac{1}{2}\,(b_{\kappa\lambda}\,B^{\kappa}_{K}\,B^{\lambda}_{L} - a_{KL}) \qquad (28a)$$

$$e_{\kappa\lambda} = \tfrac{1}{2}\,(b_{\kappa\lambda} - a_{KL}\,B^{K}_{\kappa}\,B^{L}_{\lambda}). \qquad (28b)$$

The strain e_{KL} is given in terms of (K) state coordinates, while $e_{\kappa\lambda}$ is in terms of (κ) state coordinates. The quantities $b_{\kappa\lambda}$ and a_{KL} are the metric tensors belonging with the (κ) and (K) states respectively. In particular,

$$a_{KL} = \delta_{KL} \qquad (29a)$$

while

$$b_{\kappa\lambda} = \mathbf{e}_{\kappa}\cdot\mathbf{e}_{\lambda} = B^{K}_{\kappa}\,B^{K}_{\lambda} = \begin{pmatrix} [1 + (B^{2}_{1})^{2}] & B^{2}_{2}\,B^{2}_{2} & 0 \\ B^{2}_{1}\,B^{2}_{2} & [B^{2}_{2}]^{2} & 0 \\ 0 & 0 & 1 \end{pmatrix}. \qquad (29b)$$

Since the coordinates associated with (K) → (κ) are dragged, then Equation 28, according to Equation 12b, becomes

$$e_{\kappa\lambda} = \tfrac{1}{2}\,(b_{\kappa\lambda} - a_{\kappa\lambda}). \qquad (30)$$

Consider next the strain tensor associated with the (K) → (k) coordinate transformation given by

$$e_{KL} = \tfrac{1}{2}\,(c_{kl}\,C^{k}_{K}\,C^{l}_{L} - a_{KL}) \qquad (31)$$

where c_{kl} is the metric tensor belonging to state (k). In particular

$$c_{kl} = \mathbf{e}_{k}\cdot\mathbf{e}_{l} = C^{K}_{k}\,C^{K}_{l}. \qquad (32)$$

It follows from Equations 31, 32, and 17 that $e_{KL} = 0$, as is to be expected for a coordinate transformation, since such transformations involve no distortions.

In distortions such as (k^2) → (κ^1), where dislocations are involved, Equation 28a can be rewritten as

$$e_{k^2l^2} = \tfrac{1}{2}\,(a_{\kappa^1\lambda^1}\,A^{\kappa^1}_{k^2}\,A^{\lambda^1}_{l^2} - a_{k^2l^2}) \qquad (33)$$

where

$$a_{\kappa^1\lambda^1} = a_{k^2l^2}. \qquad (34)$$

Thus, where dislocations are involved, the strain is described by a dragging of the metric, i.e., its values are kept numerically the same in states (k^2) and (κ^1). Note also that Equation 33 is a measure of the dislocation-induced strain which we may also denote as plastic strain. It does not account for the elastic distortions generated by the dislocations, i.e., we may say that the coordinates are dragged with respect to these elastic strains. Equation 33 is thus the true meaning of dislocation induced or plastic strain. However, when we write the first term in this equation as

$$d_{k^2l^2} = a_{\kappa^1\lambda^1}\,A^{\kappa^1}_{k^2}\,A^{\lambda^1}_{l^2} \qquad (35)$$

then Equation 33 can be rewritten as

$$e_{k^2l^2} = \tfrac{1}{2}\,(d_{k^2l^2} - a_{k^2l^2}) \qquad (36)$$

which is in the same form as that given in Equation 30 for the elastic strain. This, in fact, is the fundamental reason why plastic strain can be written in the same way as elastic strain [7]. In fact, if the reference state metric in Equation 33 were taken as $a_{k^2l^2} = \delta_{k^2l^2}$, then the plastic strain given by Equation 33 would be identical to the elastic strain given by Equation 30. This is a profound result since it implies that any given state of distortion can be described either in terms of classical elasticity, i.e., Riemannian geometry, or in terms of dislocation, i.e., non-Riemannian

geometry. This is also the fundamental reason why any given elastic distortion can be described in terms of some suitable continuous distribution of dislocations [8, 9].

In the case of the tearing process $(K) \rightarrow (k^3)$, the strain tensor can be written as

$$e_{k^3 l^3} = \tfrac{1}{2}\,(f_{k^3 l^3} - a_{k^3 l^3}) \tag{37}$$

where $f_{k^3 l^3}$ is the metric tensor associated with the (k^3) state and may be written

$$f_{k^3 l^3} \equiv c_{kl} \tag{38}$$

as given by Equation 32.

4. Burgers circuit, torsion tensor and anholonomic object associated with a two-phase interface

A Burgers circuit can now be associated with the fully coherent boundary of Fig. 1 with a Burgers vector or closure failure b^κ given by the following line integral [10, 11]

$$b^\kappa = -\oint B^\kappa_K \, dx^K. \tag{39}$$

It is important to note that the above integration path must be taken with respect to the initial or perfect state of the crystal. Such a circuit is shown by the path 1–2–3–4–5–6–1 in Fig. 5. More specifically, Equation 39 can be written as

$$\begin{aligned} b^2_\kappa = &-B^2_1 \underset{6-2}{\Delta x^1} - B^2_2 \underset{2-3}{\Delta x^2} - B^2_1 \underset{3-5}{\Delta x^1} \\ &- B^2_2 \underset{5-6}{\Delta x^2} = 0 \end{aligned} \tag{40}$$

and follows from Equation 12b. The quantities $\underset{6-2}{\Delta x^1}$, etc., in the above equation are simply the distances from 6 to 2, etc., in Fig. 5. In the case of the dislocated (k) and torn (k^3) states, we can write, similar to Equation 39

$$b^k = -\oint C^k_K \, dx^K \tag{41a}$$

and

$$b^{k^3} = -\oint D^{k^3}_K \, dx^K. \tag{41b}$$

In view of Equation 17a, Equation 41a becomes

$$b^2_k = -C^2_2 \underset{2-3}{\Delta x^2} - C^2_2 \underset{5-6}{\Delta x^2} \tag{42a}$$

or upon expanding

$$b^2_k = \{4\}_1 - \{4\,(1/V)\}_2 = (4/V)(V-1) = -1. \tag{42b}$$

This corresponds to the dotted closure failure 3′–2′ in Fig. 2 associated with the extra half-plane included within the Burgers circuit. In view of Equation 24b, Equation 41b gives

$$b^2_{k^3} \equiv b^2_k \tag{43}$$

In terms of Fig. 7, this closure failure is given as the dotted vector 3′–2′, and corresponds to the width of the gap generated by the tearing process. Alternately, this gap may be viewed as the resultant of the total amount of new free surface created by the tearing process, i.e., the vectors 3′–4′, 4′–1′, and 1′–2′. The free surface lengths 4′–3′ and 2′–1′ can be thought of as cancelling with one another.

For the (κ^1) state configuration of Fig. 4, we may write

$$b^{\kappa^1} = -\oint A^{\kappa^1}_{k^2} \, dx^{k^2}. \tag{44}$$

In view of Equation 14, the last expression can be expanded to give

$$b^2_{\kappa^1} = -A^2_2 \underset{2-3}{\Delta x^2} - A^2_2 \underset{5-6}{\Delta x^2} = 4. \tag{45}$$

This closure failure corresponds to the four shaded half planes within the Burgers circuit of Fig. 4. The (k^4) state of Fig. 8 can in turn be generated by a tearing of the (κ^1) state to give

$$b^{k^4} = -\oint D^{k^4}_{\kappa^1} \, dx^{\kappa^1} \tag{46}$$

where

$$D^{k^4}_{\kappa^1} = C^k_K \tag{47}$$

as given by Equation 17a. Expansion of Equation 46 yields

$$\begin{aligned} b^2_{k^4} = &-D^2_1 \underset{6-2}{\Delta x^1} - D^2_2 \underset{2-3}{\Delta x^2} \\ &- D^2_1 \underset{3-5}{\Delta x^1} - D^2_2 \underset{5-6}{\Delta x^2} \end{aligned} \tag{48a}$$

or still more simply in terms of Fig. 4

$$\begin{aligned} b^2_{k^4} &= 0 - (5/4)\,16 - 0 - (-16 - 4) \\ &= -4 + 4. \end{aligned} \tag{48b}$$

The last equation simply states that the closure failures associated with the four dislocations in Fig. 8 are just balanced by the four closure failures associated with the gaps generated by the tearing process.

The line integral given by Equation 41a can now be converted into a surface integral by means

of Stokes' theorem [12] to obtain an alternate representation of b^k given by

$$b^k = -\int_s \partial_{[L} C^k_{K]} \, dF^{LK}$$

$$= -\int_s \tfrac{1}{2} [\partial_L C^k_K - \partial_K C^k_L] \, dF^{LK} \quad (49)$$

where ∂_L denotes the operation $\partial/\partial x^L$. For the specific component $\underset{k}{b}{}^2$, Equation 49 can be written as

$$\underset{k}{b}{}^2 = -\int_s \partial_1 C^2_2 \, dF^{12} \quad (50a)$$

which from Equation 17a gives

$$\underset{k}{b}{}^2 = \left\{ \int_{-\infty}^{+\infty} \delta(\underset{K}{x}{}^1) \, dx^1 \int dx^2 \right\}_1 - \left\{ \frac{1}{V} \int_{-\infty}^{+\infty} \delta(\underset{K}{x}{}^1) \, dx^2 \int dx^2 \right\}_2 \quad (50b)$$

where the following relations have been utilized

$$\partial_1 H(-\underset{K}{x}{}^1) = -\delta(\underset{K}{x}{}^1) \quad (51a)$$

and

$$\partial_1 H(+\underset{K}{x}{}^1) = +\delta(\underset{K}{x}{}^1) \quad (51b)$$

where $\delta(\underset{K}{x}{}^1)$ is the Dirac delta function, which is zero for $\underset{K}{x}{}^1 \neq 0$. This function also satisfies the following relation

$$\int_{-\infty}^{+\infty} \delta(\underset{K}{x}{}^1) \, dx^1 = 1 \quad (52)$$

so that for the specific Burgers circuit of Fig. 5, Equation 50b gives

$$\underset{k}{b}{}^2 = \{4\}_1 - \{4\,(1/V)\}_2 \quad (53)$$

which is identical to that given by Equation 42b.

The surface integral of Equation 49 can be rewritten in a second form as

$$b^k = -\int_s \tfrac{1}{2} C^L_m C^K_l \, [\partial_L C^k_K - \partial_K C^k_L] \, dF^{ml} \quad (54a)$$

or more compactly as

$$b^k = -\int_s S_{\dot{m}\dot{l}}{}^k \, dF^{ml} \quad (54b)$$

where the quantity $S_{\dot{m}\dot{l}}{}^k$ is termed the torsion tensor, and can be written as [5]

$$S_{\dot{m}\dot{l}}{}^k = \tfrac{1}{2} C^L_m C^K_l \, [\partial_L C^k_K - \partial_K C^k_L]. \quad (55)$$

As first pointed out by Kondo [13], $S_{\dot{m}\dot{l}}{}^k$ is a measure of the dislocation content of a crystal. In particular, we may write for the specific component

$$\underset{k}{S}{}^{\dot{1}\dot{2}}_{\dot{2}} = \tfrac{1}{2} C^1_1 C^2_2 \, \partial_1 C^2_2$$

$$= \{-\tfrac{1}{2} \delta(\underset{k}{x}{}^1)\}_1 + \{\tfrac{1}{2} \delta(\underset{k}{x}{}^1)\}_2. \quad (56)$$

When this component is substituted into Equation 54b, we again obtain the same result as that given by Equation 53.

For the torn (k^3) state crystal, Equation 41b can be converted to a surface integral to give

$$b^{k^3} = -\int_s \tfrac{1}{2} D^L_{m^3} D^K_{l^3} \, [\partial_L D^{k^3}_K - \partial_K D^{k^3}_L] \, dF^{m^3 l^3} \quad (57a)$$

or more compactly as

$$b^{k^3} = \int_s \Omega^{k^3}_{m^3 l^3} dF^{m^3 l^3} \quad (57b)$$

where $\Omega^{k^3}_{m^3 l^3}$ is termed the anholonomic object and may be written as [4, 14]

$$\Omega^{k^3}_{m^3 l^3} = -\tfrac{1}{2} D^L_{m^3} D^K_{l^3} \, [\partial_L D^{k^3}_K - \partial_K D^{k^3}_L]. \quad (58)$$

It is apparent that

$$\underset{k}{S}{}^{\dot{1}\dot{2}}_{\dot{2}} \equiv -\underset{k^3}{\Omega}{}^2_{12} \quad (59)$$

from which it follows that

$$\underset{k^3}{b}{}^2 = \underset{k}{b}{}^2. \quad (60)$$

Continuing with these arguments, the line integral of Equation 44 can be rewritten as

$$b^{\kappa^1} = -\int_s S_{\dot{\mu}^1 \dot{\lambda}^1 \kappa^1} \, dF^{\mu^1 \lambda^1} \quad (61a)$$

where

$$S_{\dot{\mu}^1 \dot{\lambda}^1 \kappa^1} \equiv \tfrac{1}{2} A^{l^2}_{\mu^1} A^{k^2}_{\lambda^1} \, [\partial_{l^2} A^{\kappa^1}_{k^2} - \partial_{k^2} A^{\kappa^1}_{l^2}] \quad (61b)$$

or for the specific component

$$\underset{\kappa^1}{S}{}^{\dot{1}\dot{2}}_{\dot{2}} \equiv \underset{k}{S}{}^{\dot{1}\dot{2}}_{\dot{2}} \quad (62)$$

which, when substituted into Equation 61a, gives $\underset{\kappa^1}{b}{}^2 = 4$, i.e., the same value as that obtained from

the line integral method which led to Equation 45.

Finally, for the torn and dislocated (k^4) state, Equation 46 can be rewritten as

$$b^{k^4} = -\int_S [S_{\dot{m}^4\dot{1}^4}{}^{k^4} - \Omega^{k^4}_{\dot{m}^4\dot{1}^4}]\, dF^{m^4 1^4} \quad (63)$$

where, similar to the results of Equation 48b, $b^2_{k^4} = 0$. This arises since

$$S_{\dot{1}\dot{2}}{}^2_{k^4} = \Omega^2_{k^4 12}. \quad (64)$$

The above is an important relation and is, in fact, the basis of the naturalization process [13]. Verbally, it states that the gaps or free surfaces generated by the tearing process, and which are measured by Ω^2_{12}, just balance the extra half planes due to the dislocations, and which are measured by $S_{\dot{1}\dot{2}}{}^2$. It is, in fact, the equality of Equation 64 which has enabled Zorawski [14] to base his theory of dislocations almost exclusively on the anholonomic object, rather than the torsion tensor.

It is apparent from the concept of dragged cordinates that $S_{\dot{\mu}\dot{\lambda}}{}^{\kappa} = \Omega^{\kappa}_{\mu\lambda} = 0$. This same result can also be shown to hold when non-dragged coordinates are employed, i.e., B^{K}_{κ} as given by Equation 5, as well as its inverse are used. The component of interest becomes

$$\Omega^2_{\kappa 12} = \tfrac{1}{2} B^1_1 B^2_2 [\partial_1 B^2_2 - \partial_2 B^2_1] \quad (65)$$

which, according to Equation 8, is zero. Note that in the limiting case of the (κ) state when a in Equation 11 goes to ∞ so as to generate the (k^3) state

$$\Omega^2_{k^3 12} = \tfrac{1}{2} D^1_1 D^2_2 \partial_1 D^2_2. \quad (66)$$

This is an important result since it distinguishes the torn (k^3) state from the elastically distorted (κ) state.

In concluding this section, we have arrived at the very important result that the coincidence site lattice provides the reference coordinate system by which a dislocated state may be eliminated, i.e., the coordinate transformation (k) $\rightarrow$ (k^2); or by which an elastically distorted state may be represented by dislocations, i.e., the coordinate transformation (κ) $\rightarrow$ (κ^1). These results will next be extended in the following sections to include the still more complex case of grain boundaries.

5. Distortions associated with a symmetric tilt boundary

Let us now consider the (K^2) state reference crystal shown in Fig. 9a. Such a crystal can be uniformly bent to generate the (κ^2) state illustrated in Fig. 9b. In order to eliminate the elastic strains associated with the bent crystal, it may be torn as illustrated in Fig. 10a to generate the (k^5) state. The tearing is seen to create a pair of free surfaces $4'$–1 and 1–$4'$. If now extra matter is added to the torn state so as to create the symmetric tilt boundary shown in Fig. 10b, a dislocated (k^6) state is obtained. The (K^2), (κ^2), (k^5), and (k^6) states may be viewed as the counterparts of the (K), (κ), (k^3), and (k) states respectively associated with the two-phase interface. The open circles within the grain boundary of Fig. 10b correspond to coincidence sites and are seen to generate a coincidence site lattice common to both grains and which is denoted by dotted lines [1]. For greater clarity, this coincidence site lattice is again reproduced in Fig. 11. It has a unit cell edge length a_{oc} and will be designated as the (k^7) state representation of the grain boundary. The coincidence site lattice can be further subdivided into a smaller sublattice of dimensions a_{ocs}, and will be designated as the (k^8) state representation of the grain boundary. It is also convenient to define yet another lattice of edge length a_{oB} which will be designated as state (k^9). The corres-

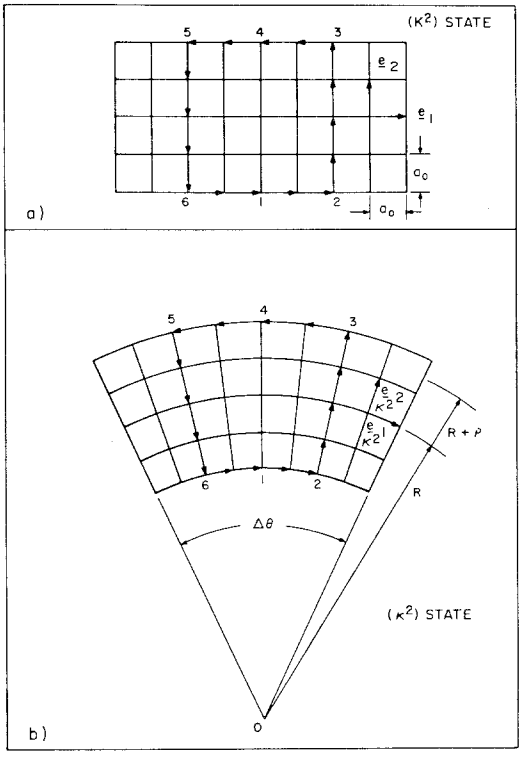

Figure 9 Uniform bending: (a) Initial state, (b) Final state.

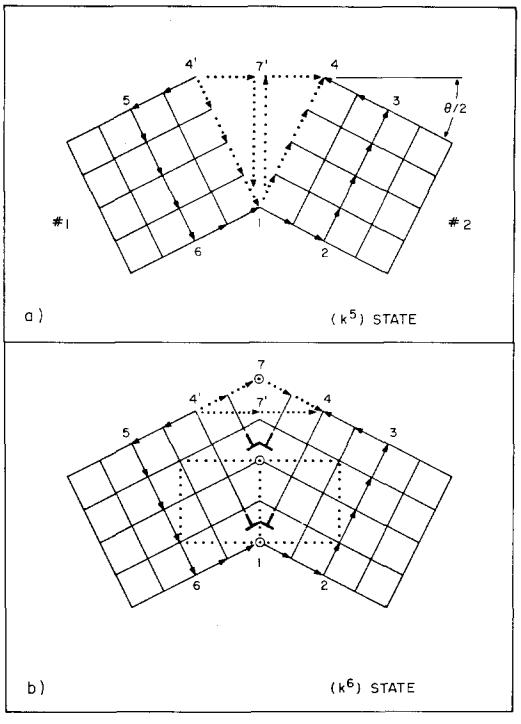

Figure 10 (a) Configuration generated by tearing of the bent state shown in Fig. 9b. (b) Symmetric tilt boundary of misorientation $\theta = 53.1°$ generated from the (k^5) state by addition of extra matter.

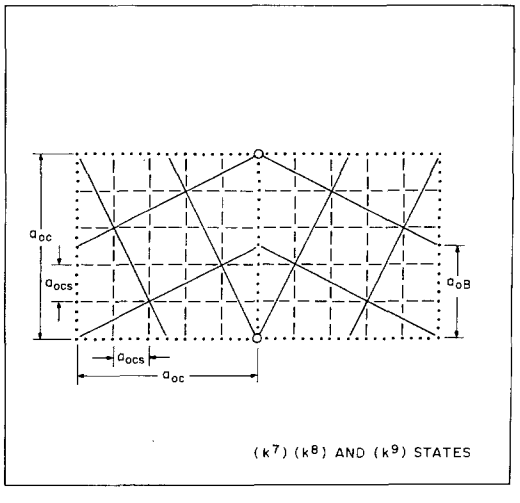

Figure 11 Coincidence site lattice and sublattice associated with the grain boundary of Fig. 10b.

pondence of Fig. 11 with that in Fig. 3 is immediately apparent.

The uniformly bent (κ^2) state can be generated from the (K^2) state via the following distortion

$$B_{\kappa^2}^{K^2} = \begin{pmatrix} \frac{R}{R+\rho}\cos\theta/2 & -\frac{R}{R+\rho}\sin\theta/2 & 0 \\ \sin\theta/2 & \cos\theta/2 & 0 \\ 0 & 0 & 1 \end{pmatrix} \tag{67}$$

where R is the radial distance to the neutral axis, while ρ is a radial distance measured with respect to this axis. The angle of rotation $\theta/2$ is measured with respect to the vertical axis. We can next form the torn state from either the (κ^2) or (K^2) states. Choosing the latter, the distortion tensor can be written as

$$D_{k^5}^{K^2} = \{{}_1D_{k^5}^{K^2} H(-x_{K^2}^1)\}_1 + \{{}_2D_{k^5}^{K^2} H(+x_{K^2}^1)\}_2 \tag{68}$$

where

$${}_1D_{k^5}^{K^2} = \begin{pmatrix} \cos\theta/2 & \sin\theta/2 & 0 \\ -\sin\theta/2 & \cos\theta/2 & 0 \\ 0 & 0 & 1 \end{pmatrix} \tag{69a}$$

and

$${}_2D_{k^5}^{K^2} = \begin{pmatrix} \cos\theta/2 & -\sin\theta/2 & 0 \\ \sin\theta/2 & \cos\theta/2 & 0 \\ 0 & 0 & 1 \end{pmatrix}. \tag{69b}$$

The above distortions are simply rigid rotations of Grains 1 and 2, while the Heaviside functions in Equation 68 are of the same form as those given by Equations 16. Dragged coordinates could also have been used to describe the $(K^2) \rightarrow (k^5)$ transformation; however, in this case, Equation 68 would have to be rewritten as

$$A_{k^5}^{K^2} = \{\delta_{k^5}^{K^2} H(-x_{K^2}^1)\}_1 + \{\delta_{k^5}^{K^2} H(+x_{K^2}^1)\}_2. \tag{70}$$

It is next possible to generate the (k^6) state from (K^2) by means of the following distortion

$$A_{K^2}^{k^6} = \{{}_1A_{K^2}^{k^6} H(-x_{K^2}^1)\}_1 + \{{}_2A_{K^2}^{k^6} H(+x_{K^2}^1)\}_2 \tag{71}$$

where

$${}_1A_{K^2}^{k^6} \equiv {}_1D_{K^2}^{k^5}/\cos\theta/2 = \begin{pmatrix} 1 & -\tan\theta/2 & 0 \\ \tan\theta/2 & 1 & 0 \\ 0 & 0 & 1 \end{pmatrix} \tag{72a}$$

and

$$A^{k^6}_{K^2} = D^{k^5}_{K^2}/\cos\theta/2 = \begin{pmatrix} 1 & \tan\theta/2 & 0 \\ -\tan\theta/2 & 1 & 0 \\ 0 & 0 & 1 \end{pmatrix}. \quad (72b)$$

This particular deformation may be visualized as relating to a volume shear which produces the material that occupies the wedge 1–4–7–4′–1 in Fig. 10b.

The (k^9) state lattice can be viewed as being generated from the (K^2) state by means of the following distortion:

$$A^{k^9}_{K^2} = \frac{1}{\cos\theta/2}\,\delta^{k^9}_{K^2} \quad (73a)$$

or in terms of dragged coordinates

$$A^{k^9}_{K^2} = \delta^{k^9}_{K^2}. \quad (73b)$$

The coincidence site lattice (k^7) can in turn be derived from the (k^9) state by means of the following coordinate transformation

$$C^{k^7}_{k^9} = \left(\frac{1}{M}\right)\delta^{k^7}_{k^9} \quad (74)$$

where M, along with another integer N, are defined as [1]

$$\tan\theta/2 = N/M. \quad (75)$$

In the case of Fig. 10b, $N = 1$ and $M = 2$. Since [1]

$$a_{ocs} = \frac{a_{oc}}{(N^2+M^2)} \quad (76)$$

the (k^8) state may be related to the (k^7) state as follows

$$C^{k^8}_{k^7} = (N^2+M^2)\,\delta^{k^8}_{k^7}. \quad (77)$$

This (k^8) state representation of the grain boundary is shown in more detail in Fig. 12a. It also follows from inspection of Equations 73a and 71 that the (k^6) and (k^9) states represent the same distortions, but expressed in terms of different coordinate frames, i.e., they can be brought into correspondence with one another by rigid rotations of $\theta/2$. Similar to Equation 71, the (K^2) state can be converted to the (k^{10}) state coordinates shown in Fig. 12b by writing

$$C^{k^{10}}_{K^2} = \{C^{k^{10}}_{1\,K^2} H(-x^1_{K^2})\}_1 + \{C^{k^{10}}_{2\,K^2} H(+x^1_{K^2})\}_2 \quad (78)$$

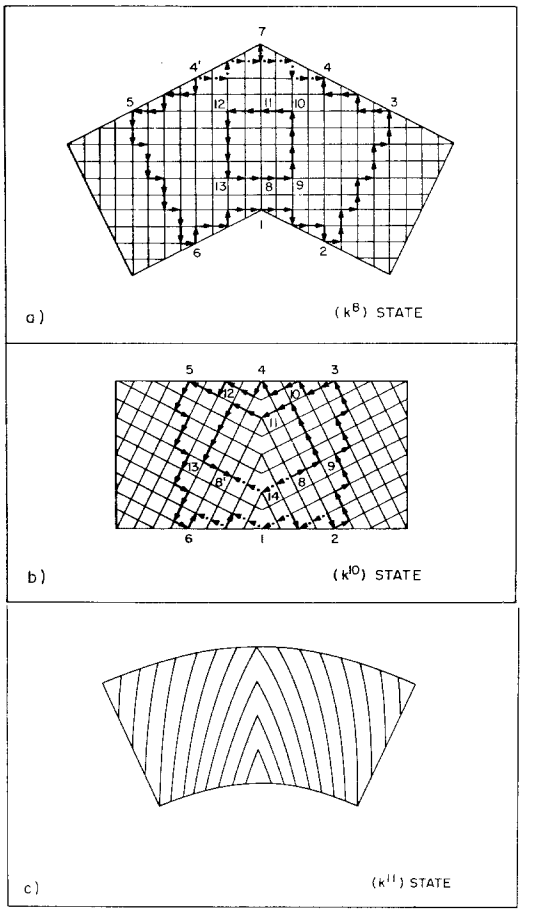

Figure 12 Alternate representations of: (a) The (k^6) state of Fig. 10b; (b) The (K^2) state of Fig. 9a; (c) The (κ^2) state of Fig. 9b.

where

$$C^{k^{10}}_{1\,K^2} \equiv NA^{k^6}_{2\,K^2} \quad (79a)$$

and

$$C^{k^{10}}_{2\,K^2} \equiv NA^{k^6}_{1\,K^2}. \quad (79b)$$

Finally, we can represent the uniformly bent (κ^2) state configuration in terms of the (k^{11}) state configuration illustrated in Fig. 12c by again employing a transformation of the type given by Equation 78. Here, however, $A^{k^2}_{K^2}$ varies smoothly with θ. Thus, as in the case of the (κ) and (κ^1) states of Figs. 1 and 4 respectively, Fig. 12 also shows that any state, whether distorted or not, may be represented in terms of a dislocated, i.e., a non-Riemannian, state or in terms of a non-dislocated, i.e., Riemannian, state. This would at first appear to contradict the concept that plastic deformation is associated with dislocations. However, from what we have seen so far, in order for there to be plastic deformation, a true distortion must occur in which the metric is dragged along,

i.e., $A^{K^6}_{K^2}$. The fact that a dislocated state can be generated from a non-dislocated state via a coordinate state transformation, i.e., $C^{K^1}_{K}$ simply means that dislocations are not always associated with plastic deformation, but may also represent elastic distortions.

6. Burgers circuit and associated tensor quantities associated with a symmetric tilt boundary

The closure failure associated with the creation of the pair of free surfaces in Fig. 10a can be written as

$$b^{k^{5'}} = \oint D^{k^{5'}}_{K^2} dx^{K^2} \tag{80}$$

which in conjunction with Equations 68 and 69 gives

$$b^1_{k^{5'}} = \{4a_0 \sin\theta/2\}_1 + \{4a_0 \sin\theta/2\}_2 \tag{81a}$$

and

$$b^2_{k^{5'}} = \{-4a_0 \cos\theta/2\}_1 + \{4a_0 \cos\theta/2\}_2 \tag{81b}$$

or in terms of Fig. 10a

$$b^1_{k^{5'}} = \{\Delta x^1\}_{1\atop 4'-7'} + \{\Delta x^1\}_{2\atop 7'-4} \tag{82a}$$

while

$$b^2_{k^{5'}} = \{\Delta x^2\}_{1\atop 7'-1} + \{\Delta x^2\}_{2\atop 1-7'}. \tag{82b}$$

The above two quantities are simply the components of the surface vectors

$$b^2_{k^5} = \{\Delta x^2\}_{1\atop 4'-1} + \{\Delta x^2\}_{2\atop 1-4} \tag{83}$$

which can be obtained by substituting Equation 70 into Equation 80. The fives are primed in Equations 80–82 to emphasize the multicomponent representation of the closure failures. The unprimed notation, on the other hand, represents a coordinate system which has been dragged [4] so that the coordinates of the initial and final states remain unchanged.

For the dislocated (k^6) state of Fig. 10b, we may write

$$b^{k^6} = -\oint A^{k^6}_{K^2} dx^{K^2} \tag{84}$$

which together with Equations 71 and 72 gives

$$b^1_{k^6} = \{4 \tan\theta/2\}_1 + \{4 \tan\theta/2\}_2 \tag{85a}$$

or in terms of Fig. 10b

$$b^1_{k^6} = \{\Delta x^1\}_{1\atop 4'-7} + \{\Delta x^1\}_{2\atop 7-4}. \tag{85b}$$

If the (k^6) state were to be torn along the boundary 1–7, then Equation 84, without the minus sign, would yield

$$b^2_{k^6} = \{-4\}_1 + \{4\}_2 \tag{86a}$$

or in terms of Fig. 10b

$$b^2_{k^6} = \{\Delta x^2\}_{1\atop 7-1} + \{\Delta x^2\}_{2\atop 1-7} = 0 \tag{86b}$$

since these surfaces cancel with one another, i.e., are not free. Thus, only the net closure failure given by Equation 85a remains. This particular closure failure may be viewed as expressed in terms of local coordinates. On the other hand, if we write Equation 84 in terms of Equation 68 then the closure failure is given by the vector 4′–4 in Fig. 10b and may be considered as expressed in terms of the original (K^2) state reference system. We have thus established a complete self-consistency between Equations 41a and 41b on the one hand, for two-phase interfaces, and Equations 84 and 80 on the other hand, for grain boundaries.

The Burgers circuit in the (k^6) state can now be represented in the (k^8) state shown in Fig. 12a. This is simply a coordinate transformation given by

$$C^{k^8}_{k^6} \equiv D^{K^2}_{k^5}\left(\frac{a_{ocs}}{\sin\theta/2}\right) \tag{87}$$

where the term in parentheses follows from the fact that

$$\sin\theta/2 = a_{ocs}/a_0. \tag{88}$$

We can thus write

$$b^{k^8} = C^{k^8}_{k^6} b^{k^6} \tag{89}$$

which in view of Equation 85a gives

$$b^1_{k^8} = \{4\}_1 + \{4\}_2 = \Delta x^1_{4'-4} \tag{90a}$$

and

$$b^2_{k^8} = \{2\}_1 + \{-2\}_2 = 0. \tag{90b}$$

These closure failures are clearly shown by the dotted arrows in Fig. 12a. The closure failures given by Equation 90a bear a close resemblance to those given for the (k^5) state by Equation 82a. In both cases, they may be viewed as the vector sum of the Burgers vectors associated with the crystal lattice dislocations (CLD) of Fig. 10b. This vector sum may in turn be associated with a so-called grain boundary dislocation (GBD) [1]. In a similar

manner, the Burgers circuit of Fig. 9a may be redrawn in terms of the (k^{10}) state coordinate system shown in Fig. 12b. In this case, we may write

$$b^{k^{10}} = -\oint C^{k^{10}}_{K^2}\, dx^{K^2} \tag{91}$$

where $C^{k^{10}}_{K^2}$ is given by Equation 78. The closure failure associated with Equation 91 is shown by the eight dotted vectors between 2–6 in Fig. 12b. It is obvious from what has been said in connection with Equation 31 that a change in coordinate system cannot have associated with it a strain tensor. On the other hand, the (k^{10}) state can be generated from the (k^8) state by means of the following distortion

$$A^{k^{10}}_{k^8} = \{A^{k^{10}}_{1\,k^8} H(-x^1_{k^8})\}_1 + \{A^{k^{10}}_{2\,k^8} H(+x^1_{k^8})\}_2 \tag{92}$$

where

$$A^{k^{10}}_{1\,k^8} \equiv A^{k^6}_{2\,K^2} \tag{93a}$$

and

$$A^{k^{10}}_{2\,k^8} \equiv A^{k^6}_{1\,K^2} \tag{93b}$$

as given by Equations 72. Using the small reference circuit 8–9–10–11–12–13–8 in Fig. 12a, we may write, similar to Equation 84

$$b^{k^{10}} = -\oint A^{k^{10}}_{k^8}\, dx^{k^8} \tag{94}$$

which gives

$$b^1_{k^{10}} = \{-4 \tan \theta/2\}_1 + \{-4 \tan \theta/2\}_2 \tag{95a}$$

and

$$b^2_{k^{10}} = \{4\}_1 + \{-4\}_2 \tag{95b}$$

which in terms of the smaller Burgers cirucit in Fig. 12b can be written as

$$b^1_{k^{10}} = \{\Delta x^1\}_{1\ 14-8} + \{\Delta x^1\}_{2\ 8-14} \tag{96a}$$

and

$$b^2_{k^{10}} = \{\Delta x^2\}_{1\ 8'-11} + \{\Delta x^2\}_{2\ 11-8}. \tag{96b}$$

These relations are similar in form to those given by Equations 85 and 86. This is to be expected since the deformation which generates state (k^6) from (K^2) is just the inverse of that which generates state (k^{10}) from (k^8). It is apparent that in both these cases a plastic strain is associated with the deformation. In particular, in the former case

$$e_{K^2L^2} = \tfrac{1}{2}\,(g_{k^6l^6} A^{k^6}_{K^2} A^{l^6}_{L^2} - g_{K^2L^2}) \tag{97}$$

where $g_{K^2L^2} = \delta_{K^2L^2}$. The above relation combined with Equations 72 yields

$$e_{K^2L^2} = \begin{pmatrix} \frac{1}{2}\tan^2\theta/2 & 0 & 0 \\ 0 & \frac{1}{2}\tan^2\theta/2 & 0 \\ 0 & 0 & 0 \end{pmatrix}. \tag{98}$$

The e_{22} component in the above tensor measures the plastic strain associated with the increase in length of the line element 1–4 in Fig. 9a to 1–7 in Fig. 10b, and has been discussed in detail elsewhere [15]. It is also apparent that Equation 97 also gives the same plastic strain for the $(k^8) \rightarrow (k^{10})$ state transformation.

Once again, it should be emphasized that the coincidence site lattice or sublattice corresponds to a coordinate system which enables the dislocation content, described in terms of the original system, to be eliminated. It is assumed, however, that the boundary is perfect. If, on the other hand, the boundary is imperfect, say as would occur by the removal of some of the dislocations, we obtain the configuration shown in Fig. 13a. The corresponding representation in terms of the coincidence site lattice and sublattice is shown in Fig. 13b [16]. In terms of the former notation, it can be inferred that five dislocations are missing within the circumscribed Burgers circuit, which would otherwise make the boundary perfect. In terms of the coincidence site lattice of Fig. 13b, the Burgers circuit shows that there is an excess of ten dislocations which keeps the crystal from being perfect. Although both dislocation representations in Fig. 13 are correct, the one shown in Fig. 13b has a distinct advantage over the other in that it can be represented in terms of a finite rather small number of dislocations. It is in fact this representation which is most closely related to the so-called grain boundary dislocations observed within the electron microscope [17].

As was the case for the two-phase interface, Equation 68 can be converted to a surface integral via Stokes' theorem to give

$$b^{k^6} = -\oint A^{k^6}_{K^2}\, dx^{K^2} = -\int_s \partial_{[L^2} A^{k^6}_{K^2]}\, dF^{L^2K^2}. \tag{99}$$

For the specific component $b^1_{k^6}$, the above equation yields

$$b^1_{k^6} = -\int_s \partial_1 A^1_2\, dF^{12} \tag{100a}$$

which with Equation 71 gives

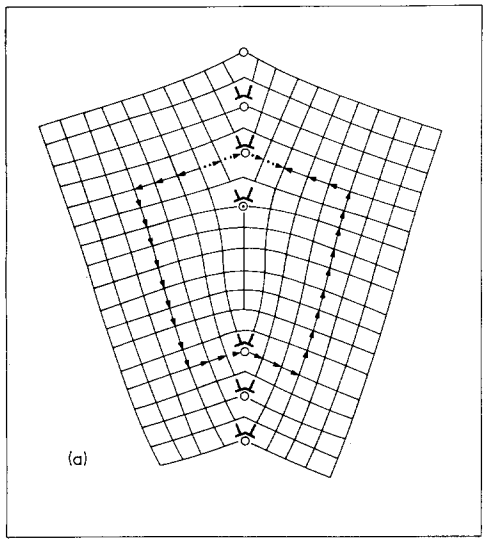

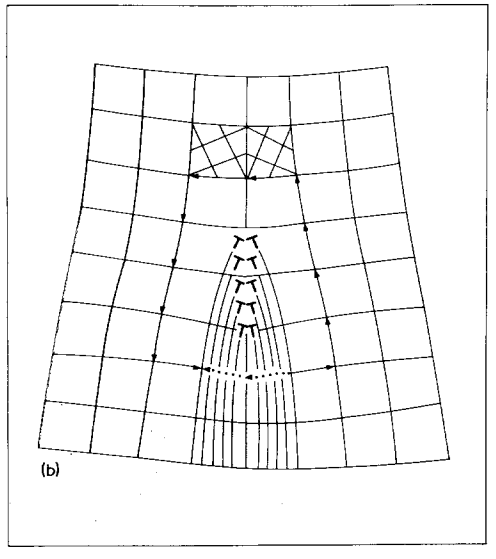

Figure 13 (a) Dislocation deficient tilt boundary of misorientation $\theta = 53.1^\circ$ represented in terms of the original crystal lattices. (b) Same boundary as that shown in (a) but represented in terms of the coincidence site sublattice.

$$b^{1}_{k^6} = \left\{ \int_{-\infty}^{+\infty} \tan\theta/2\, \delta(x^1_{K^2})\, dx^1 \int dx^2 \right\}_1 + \left\{ \int_{-\infty}^{+\infty} \tan\theta/2\, \delta(x^1_{K^2})\, dx^1 \int dx^2 \right\}_2 . \tag{100b}$$

When integrated, the above equation reduces to the same relation as that given by Equation 85a. Equation 99 can also be written as

$$b^{k^6} = -\int_s S_{\dot{m}^6 \dot{1}^6}{}^{k^6}\, dF^{m^6 1^6} \tag{101}$$

where

$$S_{\dot{m}^6 \dot{1}^6}{}^{k^6} = \tfrac{1}{2} A^{L^2}_{m^6} A^{K^2}_{1^6} \left[\partial_{L^2} A^{k^6}_{K^2} - \partial_{K^2} A^{k^6}_{L^2} \right] \tag{102}$$

or more specifically

$$S_{k^6 \dot{1}\dot{2}}{}^{1} = \tfrac{1}{2} \left[A^1_1 A^2_2 - A^2_1 A^1_2 \right] \partial_1 A^1_2 \tag{103a}$$

which can be expanded to give

$$S_{k^6 \dot{1}\dot{2}}{}^{1} = \left\{ -\tfrac{1}{2} \tan\theta/2\, \delta(x^1_{k^6}) \right\}_1 + \left\{ -\tfrac{1}{2} \tan\theta/2\, \delta(x^1_{k^6}) \right\}_2 \tag{103b}$$

which when substituted into Equation 101 gives the same relation as that given by Equation 85a, again establishing the complete self-consistency between all of these methods. It can also be shown, similar to Equation 57b, that

$$b^{k^5} = \int_s \Omega^{k^5}_{m^5 1^5}\, dF^{m^5 1^5} \tag{104}$$

where

$$\Omega^{k^5}_{m^5 1^5} = S_{\dot{m}^6 \dot{1}^6}{}^{k^6}. \tag{105}$$

The anholonomic object may be thought of as associated with the free surfaces in Fig. 10a, while the torsion tensor is a measrue of the dislocation content as illustrated in Fig. 10b. Similar expressions can be obtained for the coincidence site lattice representations of Fig. 12. In addition, the dislocated grain boundary states can be torn so as to generate a condition given by Equation 64.

7. Some further considerations associated with internal interfaces

The torsion tensor and anholonomic object can be utilized to determine either the dislocation densities or density of newly created free surfaces by means of the following relations [5, 14, 15]

$$\alpha^{nk} = -\epsilon^{nlm} S_{l\dot{m}}{}^{k} \tag{106a}$$

and

$$\alpha^{nk} = \epsilon^{nlm} \Omega^{k}_{lm} \tag{106b}$$

where ϵ^{nlm} is the permutation tensor defined by

$$\epsilon^{nlm} = e^{nlm}/\sqrt{g} \tag{107}$$

where e^{nlm} is the permutation symbol and g is the determinant of the metric tensor. In the case of Fig. 10b, Equation 106a gives

$$\alpha^{31}_{k^6} = \{\tan\theta/2\, \delta(x^1_{k^6})\}_1 + \{\tan\theta/2\, \delta(x^1_{k^6})\}_2 \tag{108a}$$

which in terms of Fig. 10b is simply

$$\underset{k^6}{\alpha^{31}} = \left\{ \frac{\Delta x^1}{\frac{4'-7}{\Delta x^2}} \right\}_1 + \left\{ \frac{\Delta x^1}{\frac{7-4}{\Delta x^1}} \right\}_2 . \qquad (108b)$$

In a similar manner, Equation 106b gives

$$\underset{k^5}{\alpha^{32}} = \{-\delta(\underset{k^5}{x^1})\}_1 + \{\delta(\underset{k^5}{x^1})\}_2 \qquad (109)$$

where $\underset{k^5}{\alpha^{32}}$ may be thought of as a measure of the newly created free surface density in Fig. 10a.

A final item of interest, and one which seems to have not been given much attention in the past, corresponds to what may be termed a law of conservation of the Burgers vector. This states that the sum of the Burgers vectors in a given manifold must always equal zero. This is also equivalent to saying that dislocations should always be created in pairs of opposite sign. Fig. 4 would at first seem to contradict this law since all of the dislocations shown therein are of the same sign. However, this particular picture is incomplete since surface dislocations must be added to eliminate the surface tractions [9, 18], resulting from the internal dislocations. These surface dislocations may be more easily seen by considering the finite body of Fig. 4 imbedded in an infinite medium such as shown in Fig. 14. The overall distortion may then be described by a single vertical set of dislocations as well as two sets of horizontal dislocations. The horizontal dislocations may be viewed as the surface dislocations since they define a surface along which the surface tractions vanish. The infinite body can thus be cut along these surfaces to generate the (κ^1) state of Fig. 4. Note now that when a Burgers circuit is taken along this entire array, as shown in Fig. 14, the positive and negative closure failures add up to zero, in accordance wtih the previously stated law. The surface dislocations may also be viewed as those providing the image forces to the free surfaces. This is a very powerful concept and has been used to solve a number of crack problems [18]. No image dislocations are present for the (k) state of Fig. 2, since they may be viewed as having moved from the surface to the interface to completely annul the stress fields of the virtual dislocations shown dotted. This will always manifest itself when a coincidence site lattice can be constructed, i.e., the transformation from state (k) to (k^2) or from (k^6) to (k^8).

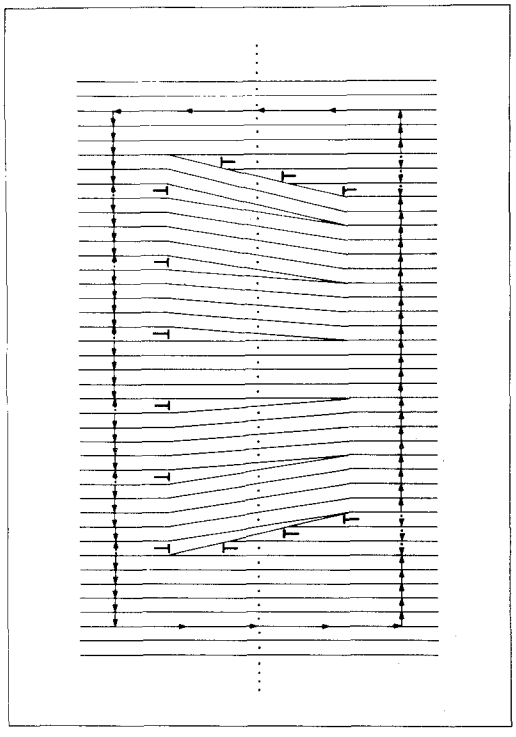

Figure 14 Modification of Fig. 4 in which extra material has been added to the top and bottom faces.

8. Summary and conclusions

Simple two-phase interfaces and tilt-type grain boundaries have been analysed in terms of their coincidence site lattices. It is shown that these particular lattices provide a new reference whereby an elastic distortion or else a perfect lattice may be described in terms of dislocations. On the other hand, the coincidence site lattice can be used to represent an originally dislocated space as dislocation free. The various tensor quantities, such as distortion, metric, strain, torsion, etc., have all been defined and analysed with respect to both the original crystal lattice as well as the corresponding coincidence site lattice. It is shown that the flexibility involved in transforming from a dislocated to a non-dislocated state and vice versa provides a powerful method for solving various problems in continuum mechanics.

Acknowledgements

The author would like to express his appreciation to Dr R. deWit of the Metallurgy Division and Institute for Materials Research of The National Bureau of Standards, Washington, DC as well as to Dr K. Jagannadham of the Engineering Materials

Group and Department of Mechanical Engineering of the University of Maryland for a number of enlightening discussions. Financial support for the present study was provided by the National Science Foundation under Grant no. DMR-7202944.

References

1. M. J. MARCINKOWSKI and K. SADANANDA, *Acta Crystall.* **A31** (1975) 280.
2. M. J. MARCINKOWSKI, K. SADANANDA and W. H. CULLEN, Jr., *ibid.* **A31** (1975) 292.
3. M. J. MARCINKOWSKI, "Fundamental Aspects of Dislocation Theory," Vol. 1, edited by J.A. Simmons, R. deWit and R. Bullough, (NBS Special Publication no. 317, 1970) p. 531.
4. J. A. SCHOUTEN, "Ricci-Calculus" (Springer-Verlag, Berlin, 1954).
5. E. KRÖNER, "Kontinuumstheorie Der Versetzungen Und Eigenspannungen" (Springer-Verlag, Berlin, 1958).
6. Y. C. FUNG, "Foundations of Solid Mechanics" (Prentice Hall, Inc., New Jersey, 1965).
7. K. H. ANTHONY, "Fundamental Aspects of Dislocation Theory," NBS Vol. 1, edited by J.A. Simmons, R. deWit and R. Bullough, (Special Publication No. 317, 1970) p. 637.
8. K. JAGANNADHAM and M. J. MARCINKOWSKI, *J. Appl. Phys.*, **48** (1977) 3788.
9. K. JAGANNADHAM and M. J. MARCINKOWSKI, *Phys. Stat. Sol. (a)* **50** (1978).
10. E. KRÖNER, *Arch. Rat. Mech. Anal.* **4** (1959) 273.
11. J. P. HIRTH and J. LOTHE, "Theory of Dislocations" (McGraw–Hill, New York, 1968).
12. J. A. SCHOUTEN, "Tensor Analysis for Physicists" (Clarendon Press, London, 1951).
13. K. KONDO, "Memoirs of the Unifying Study of the Basic Problems in Engineering Sciences by Means of Geometry" (Gakujutsu Bunken Fukyu-kai, Tokyo, 1955) p. 458.
14. M. ZORAWSKI, "Théorie Mathématique des Dislocations," (Dunod, Paris, 1967).
15. M. J. MARCINKOWSKI, *Phys. Stat. Sol.* **a38** (1976) 223.
16. M. J. MARCINKOWSKI and K. SADANANDA, *ibid.* **a18** (1973) 361.
17. W. F. TSENG, M. J. MARCINKOWSKI, and E. S. DWARAKADASA, *J. Mater. Sci.* **9** (1974) 41
18. M. J. MARCINKOWSKI and E. S. P. DAS, *Int. J. Fracture* **10** (1974) 181.

Received 22 May and accepted 26 May 1978.